Cryogenics 83 (2017) 50–56

Contents lists available at ScienceDirect

Cryogenics

journal homepage: www.elsevier.com/locate/cryogenics

Technical note

Cryogenic design of liquid-nitrogen circulation system for long-length HTS cables with altitude variation

Ho-Myung Chang [a,*], Ki Nam Ryu [a], Hyung Suk Yang [b]

[a] Hong Ik University, Seoul 121-791, Republic of Korea
[b] Korea Electric Power Corporation, Daejeon 305-760, Republic of Korea

ARTICLE INFO

Article history:
Received 30 December 2016
Received in revised form 7 February 2017
Accepted 13 February 2017
Available online 27 February 2017

Keywords:
Cryogenic design
Liquid nitrogen
Circulation
HTS cables
Altitude variation

ABSTRACT

Liquid-nitrogen (LN_2) circulation systems with altitude variation are investigated and designed for application to practical long-length HTS cables. This study is motivated by the KEPCO's immediate plan to install new HTS cables in existing utility tunnels including inclined and vertical sections. The distribution of pressure and temperature along the LN_2 circulation loop is examined for various geographic conditions, taking into account the gravitational effect of altitude variation. The cryogenic cooling requirements are defined in terms of the pressure and temperature of LN_2, and a design process is graphically demonstrated on phase diagram. It is concluded that the LN_2 flow rate along the cable with altitude variation should be carefully determined with the constraints on pressure and temperature, and the proposed graphical method is useful in the design.

1. Introduction

HTS (high-temperature superconductor) cables are under worldwide development for power transmission with a great energy density [1–7]. The KEPCO (Korea Electric Power Corporation) is one of the leading groups, who has made a recent progress to demonstrate 500 m 80 kV DC cables [7] and 1 km 154 kV AC cables in Jeju. As next step, the KEPCO plans to install new 23 kV AC HTS cables in existing underground utility tunnels connecting two substations. This plan has been motivated by the advantage of HTS cables to increase the transmission capacity without costly construction of new tunnels in urban area. The installation of HTS cables in the existing tunnels, however, accompanies the strict geographical constraints not only on the cable length, but also on their altitude variation. The actual distance between two adjacent substations is 1–3 km and the altitude changes up to 50 m in vertical height along the tunnel. Unlike conventional cables, the altitude variation could be important in cryogenic design, since liquid nitrogen (LN_2) is used as coolant.

The cryogenic cooling system under design is schematically shown in Fig. 1. An HTS cable (3 cores in 1 cryostat) is installed in a tunnel connecting two terminals. LN_2 is pumped along the HTS cable, and then flows back through a return pipe. The thermal load of entire system is removed by a Brayton refrigerator in the cooling facility building. The LN_2 circulation loop can be plotted as a counterclockwise cycle on phase (P-T) diagram shown in Fig. 2, where the pressure drop (ΔP) and temperature rise (ΔT) should be recovered by the pump and refrigerator, respectively [8]. When the flow rate is relatively low, ΔP is small and ΔT is large so that the cycle is horizontally sharp. As the flow rate becomes higher, on the contrary, ΔP gets larger and ΔT gets smaller so that the cycle becomes tall and slim.

If there is no or negligibly small variation in elevation, the cryogenic design is focused mainly on the inlet and exit states of HTS cable. For the cables with significant altitude variation, however, the LN_2 process on phase diagram may not be simply linear because of the gravitational effect. Fig. 3 shows an example of geographic layout of the underground tunnel to install the HTS cable in. The horizontal distance between two terminals is 1.5 km, but the cable length should be over 1.6 km, because there is a 50 m deep section (②-③-④-⑤) to make a detour under subway line. There is also an inclined section ⑥-⑦, as Terminal B is located at an elevation of 30 m below Terminal A.

Little attention has been paid so far to the gravitational effect in cryogenic design, because the altitude variation in demonstration cables is negligibly small. Demko and Hassenzahl [9] presented a study on thermal management for 20 km long cable design, where different coolants (LN_2, gaseous hydrogen and helium) were compared by including the effect of elevation change.

This study is proposed to investigate the thermal and hydraulic behavior of LN_2 flow along the HTS cables, taking into account the

* Corresponding author.
E-mail address: hmchang@hongik.ac.kr (H.-M. Chang).

http://dx.doi.org/10.1016/j.cryogenics.2017.02.004
0011-2275/

Nomenclature

A	cross-sectional area
C_p	specific heat at constant pressure
D	inner diameter of LN_2 cryostat
d	outer diameter of cable core
D_h	hydraulic diameter
E	energy
f	Darcy friction factor
g	gravitational acceleration
h	specific enthalpy
K	minor loss coefficient
$\dot{m}$	mass flow rate of LN_2
P	pressure
q	heat load
q'	heat load per unit length
Re	Reynolds number
T	temperature
v	specific volume (=$1/\rho$)
z	altitude or vertical height

Greek letters

ε	surface roughness
θ	inclined angle above horizontal
ρ	density
ξ	distance along cable from terminal

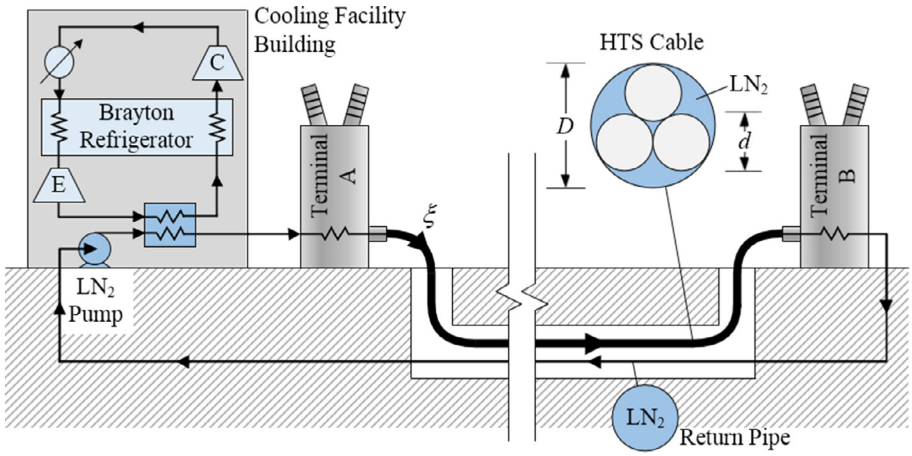

Fig. 1. Schematic of cryogenic cooling system for a long-length HTS cable to be installed in underground utility tunnel between two terminals.

gravitational effect of altitude variation. In a recent paper by the authors, the cooling requirements of HTS cables are presented in terms of LN_2 pressure and temperature [8]. The goal of this study is to combine the thermo-hydraulic analysis with the cooling requirements and verify how the altitude variation affects the cryogenic design of long-length cables.

2. Definition and analysis

2.1. Cryogenic requirements

The cryogenic cooling requirements of HTS cables are defined as a "trapezoidal" region on phase (P-T) diagram of nitrogen shown in Fig. 2 [8]. Four borders of the trapezoid are the upper or lower limits in operating pressure or temperature, as determined by the electromagnetic, thermal, or mechanical properties of cable materials and coolant.

The first and most important requirement is the upper limit of temperature for superconductivity, as indicated by the right vertical line in Fig. 2. This limit is determined by the layered structure of cable cores and the temperature-dependent electromagnetic properties of HTS tapes. The second requirement is the sub-cooling limit, shown by the curve at bottom. The sub-cooled state of LN_2 is essential for electrical insulation, because any bubbles generated by internal or external heat source should be suppressed [10]. This limit is given by a temperature margin below the boiling temperature, which is graphically a horizontal shift of the vapor-pressure curve on phase diagram. The third requirement is the lower limit of temperature to avoid the freezing of liquid, as indicated by the left vertical line. The possibility of LN_2 freeze-out is a safety issue for long-length cables, as the temperature of

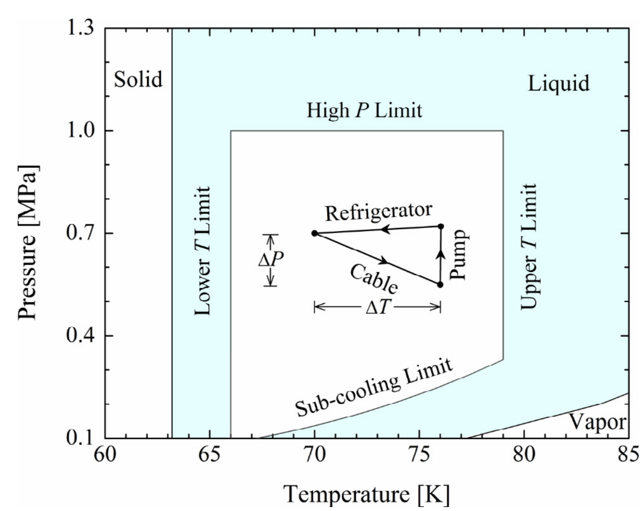

Fig. 2. A typical LN_2 cycle in trapezoidal region to show the cooling requirements on phase diagram.

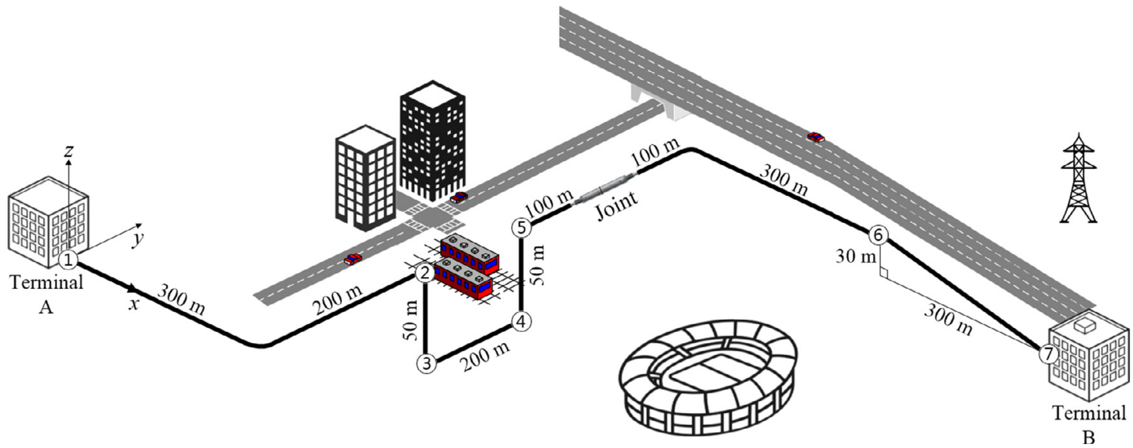

Fig. 3. An example of geographic layout for underground tunnels with vertical and inclined sections.

refrigerant (helium or neon gas in Brayton refrigerator) could be lower than the freezing point of LN_2 (63.4 K). Even though anti-freezing schemes have been developed for the sub-cooling heat exchangers [11,12], a safety margin should be secured. The last requirement is the allowable maximum pressure, as indicated by the top horizontal line. This pressure is determined by the mechanical strength of LN_2 cryostat with a safety factor.

For quantitative discussion, the four limits are selected in this design on a basis of recent KEPCO cables, as plotted in Fig. 2. The upper and lower limits of temperature are 79 K and 66 K, respectively. The sub-cooling limit is 10 K below the boiling temperature, and the high pressure limit is 1.0 MPa [9]. An important point is that the low pressure limit is not a single value, but the sub-cooling limit, which is specified as a functional relation of pressure and temperature.

2.2. Analysis and calculation model

The pressure (P) and temperature (T) of LN_2 flow along the cable with altitude variation are calculated with the momentum (modified Bernoulli) equation [13] and the energy equation, respectively. For a mass flow rate ($\dot{m}$) of LN_2 with density (ρ) and specific heat (C_p) through a cross-sectional area (A),

$$P(\xi) = P(0) - \frac{\dot{m}^2}{2\rho A^2}\left(\frac{f}{D_h}\xi + \sum_i K_i\right) - \rho g \cdot z(\xi) \tag{1}$$

$$T(\xi) = T(0) + \frac{1}{\dot{m}C_p}\left(q' \cdot \xi + \sum_i q_i\right) \tag{2}$$

where $z(\xi)$ is the vertical height expressed as a function of the distance from the terminal along the cable (ξ) as indicated in Figs. 1 and 3, and $P(0)$ and $T(0)$ are the pressure and temperature at the inlet of the cable ($\xi = 0$), respectively. In Eq. (1), D_h is the hydraulic diameter of the non-circular flow passage for 3-in-1 cable [12]

$$D_h = \frac{D^2 - 3d^2}{D + 3d} \tag{3}$$

where D and d are the inner diameter of LN_2 cryostat and the outer diameter of cable core, respectively, as shown in Fig. 1. The Darcy friction factor (f) is a function of Reynolds number (Re) and relative roughness (ε/D_h), as approximated by the implicit Colebrook-White correlation

$$\frac{1}{\sqrt{f}} = -2\log\left(\frac{\varepsilon}{3.7D_h} + \frac{2.51}{Re\sqrt{f}}\right) \tag{4}$$

Table 1
Dimension and parameters of HTS cables.

Symbol	Quantity	Values
D	Inner diameter of LN_2 cryostat	88 mm (HTS cable) 50 mm (return pipe)
d	Outer diameter of cable core	40 mm
ρ	Density of LN_2	817.9 kg/m^3
C_p	Specific heat of LN_2	2026 J/kg K
K_i	Minor loss coefficient	2.5 (terminal) 1.5 (joint) 0.5 (90° elbow)
q_i	Additional heat	400 W (each terminal)

Since the surface roughness is different for the cable core and the corrugated cryostat, a "perimeter-weighted" average [14] is used here as

$$f = \frac{f_D D + 3 f_d d}{D + 3d} \tag{5}$$

where f_D and f_d are the friction factors of cryostat [15] and cable core [16], respectively. For the round return pipe, D_h is simply its inner diameter. In Eq. (1), K_i is the minor loss coefficient for joints, elbows, or terminals located between 0 and ξ. In Eq. (2), the pressure effect on enthalpy and the potential energy according to altitude variation have been included for energy balance, as described in Appendix A. q' and q_i are the heat load per unit length (W/m) and the additional heat at terminals (W) located between 0 and ξ, respectively.

For quantitative discussion, the dimension and parameters used in this design study are listed in Table 1. The LN_2 properties are taken as the values at (75 K, 0.6 MPa) from the NIST database [17]. The hydraulic diameter of the HTS cable (D = 88 mm, d = 40 mm) is 14.2 mm from Eq. (3). Since Re is in the range of 1.1–2.8 × 10^6 (for 0.3–0.8 kg/s, as discussed later), f is nearly independent of Re, but determined by the relative roughness. For typical cable cores, ε is approximately 1 mm [16], so the friction factor (f_d) is estimated from Eq. (4).

$$f_d \approx 0.084 \tag{6}$$

For the inner surface of corrugated cryostat, Ivanov et al. [14] and Watanabe et al. [16] assumed a pipe whose mean height roughness is 0.1 mm. Upon this assumption, the friction factor (f_D) is a constant around 0.034 from Eq. (4). Weisend and Van Sciver [15] reported that f_D was 0.026–0.037 (the Fanning friction factor multiplied by 4) from their LN_2 pressure drop experiment in short-length corrugated bellows. In addition, they also stated that the measured pressure drop was roughly four times the equivalent smooth tube pressure drop, which implies that f_D could be 0.046–0.040 for Re = 1.1–2.8 × 10^6 under this flow condition.

$$0.026 \leqslant f_D \leqslant 0.046 \tag{7}$$

For conservative design, f_D is taken here as 0.046, and the averaged friction factor is finally calculated with Eq. (5) for HTS cable. The friction factor of return pipe is estimated simply for a round tube with ε = 0.1 mm.

$$f = \begin{cases} 0.068 & \text{(HTS cable)} \\ 0.023 & \text{(return pipe)} \end{cases} \tag{8}$$

Minor loss coefficients are listed as well in Table 1, even though their contribution might not be significant.

The heat load is estimated from the previous experimental data and recent progress. For 23 kV-50 MVA class cables, the expected value of ac loss per unit length is 1.0 W/m/phase [1,6,14]. It is reasonably assumed that the heat leak from ambient to vacuum-insulated cryostat is 1 W/m for the 3-phase HTS cable and 0.5 W/m for the return pipe [9]. As a result, the heat load is taken here as

$$q' = \begin{cases} 4.0\ \text{W/m} & \text{(HTS cable)} \\ 0.5\ \text{W/m} & \text{(return pipe)} \end{cases} \tag{9}$$

The additional heat is assumed to be 400 W in each terminal, which includes 270 W (=3 × 90 W) from 3-phase current leads optimized for the rated current of 2 kA [13]. The heat at joints and the viscous dissipation of LN_2 flow are small and neglected in this design.

3. Results and discussion

3.1. Effect of inclined angle

Along the HTS cable or return pipe whose inclined angle is θ above horizontal, the pressure and temperature gradients are

$$\frac{dP}{d\xi} = -\left(\frac{\dot{m}^2 f}{2\rho A^2 D_h} + \rho g \sin\theta\right) \tag{10}$$

$$\frac{dT}{d\xi} = \frac{q'}{\dot{m} C_p} \tag{11}$$

because $dz/d\xi = \sin\theta$ in Eq. (1). Combining Eq. (10) and (11), the slope of LN_2 flow on phase diagram can be expressed as

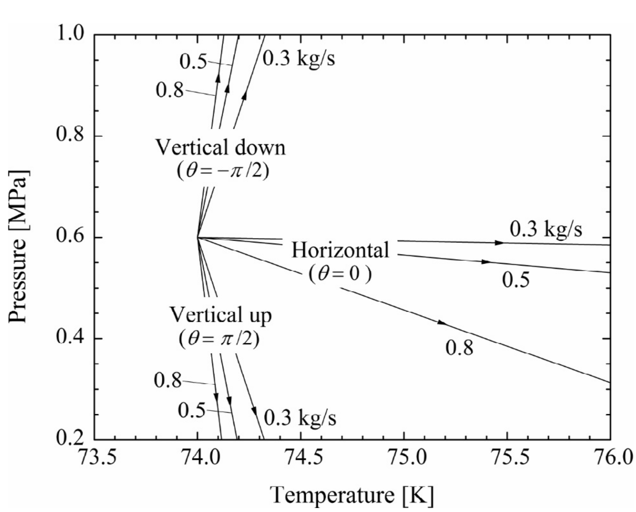

Fig. 4. Effect of inclined angle of HTS cables on the change of pressure and temperature of LN_2.

$$\frac{dP}{dT} = -\frac{\dot{m} C_p}{q'}\left(\frac{\dot{m}^2 f}{2\rho A^2 D_h} + \rho g \sin\theta\right) \tag{12}$$

which is plotted in Fig. 4. The straight lines indicate the direction of pressure and temperature change along the LN_2 flow, for example, at (0.6 MPa, 74 K).

For horizontal flows (θ = 0), the slope is always negative and relatively small in magnitude, since the temperature rise is dominant over the pressure drop. It is noted in Eq. (12) that the slope is proportional to the cube of the flow rate, when θ = 0. For vertical flows, the LN_2 process is far different, being affected by the hydrostatic pressure. In case of downward vertical flows ($\theta = -\pi/2$), the slope is positive and becomes steeper as the flow rate increases. In case of upward vertical flows ($\theta = \pi/2$), on the contrary, the slope is negative and becomes steeper as the flow rate increases.

3.2. Simple cases

The key parameter in this cryogenic design is the flow rate of LN_2, as the distribution of LN_2 pressure and temperature over the circulation loop is strongly coupled with the flow rate. As a preliminary study, seven simple cases of altitude variation over 1.5 km distance are selected and shown in Fig. 5. In each case, the LN_2 process along the HTS cable is plotted for three different values of LN_2 flow rate (0.3, 0.5, and 0.8 kg/s).

Case (a) is the simplest condition with horizontal flow only. Since there is no gravitational effect, the LN_2 process is plotted as a straight line. For an exit condition fixed at (0.4 MPa, 78 K), the cooling requirements are satisfied with any flow rate between 0.3 and 0.8 kg/s. The inlet temperature should be low if the flow rate is 0.3 kg/s, while the inlet pressure should be high if the flow is 0.8 kg/s. The decision of flow rate is a typical engineering problem, taking into consideration the economic factor about the LN_2 pump and the cryogenic refrigerator. For long-length cables, a large flow rate might be preferred to take advantage of high-temperature operation, if the price and cooling capacity of commercial refrigerators should be a major factor. According to the manufacturer's data, for example, the cooling capacity of recent Brayton refrigerators at 77 K is greater by 20% or more than the capacity at 65 K [11,18].

In Case (b), a more careful design is needed because of the ascending section near the exit. When the flow rate is 0.3 or 0.5 kg/s, the cooling requirements may be satisfied, only if the inlet pressure is set at a higher value. When the flow rate is 0.8 kg/s, however, the required inlet pressure exceeds the high pressure limit. For safe operation, the entire process may be shifted to left and down on phase diagram in order to fit in the trapezoid, as indicated by dashed lines in Fig. 5(b). In practice, it is a severe condition to supply the lower-temperature "and" higher-pressure LN_2 at the inlet of HTS cables. In Case (c), on the contrary, the inlet pressure may be set at a lower value due to the descending section near the exit. Since the pressure near the exit is recovered by gravity, the maximum allowable flow rate could be even larger than Case (a) (up to 1.0 kg/s). A key point in this case is that the LN_2 pressure has its minimum not at the exit of the cables, but at the starting point of descending section. Especially when the flow rate is 0.3 kg/s, the operating pressure should be raised above the subcooling limit, as indicated by dashed lines in Fig. 5(c).

Case (d) and Case (e) include a descending and ascending section near the inlet, respectively. In fact, these are the same geographic layouts as Case (b) and Case (c), respectively, but the direction of LN_2 flow is opposite. In Case (d), the pressure increases along the descending flow near the inlet and the flow rate may be selected over a wide range (0.3–1.0 kg/s). It is noted as well that the LN_2 pressure has the maximum not at the inlet of the cables,

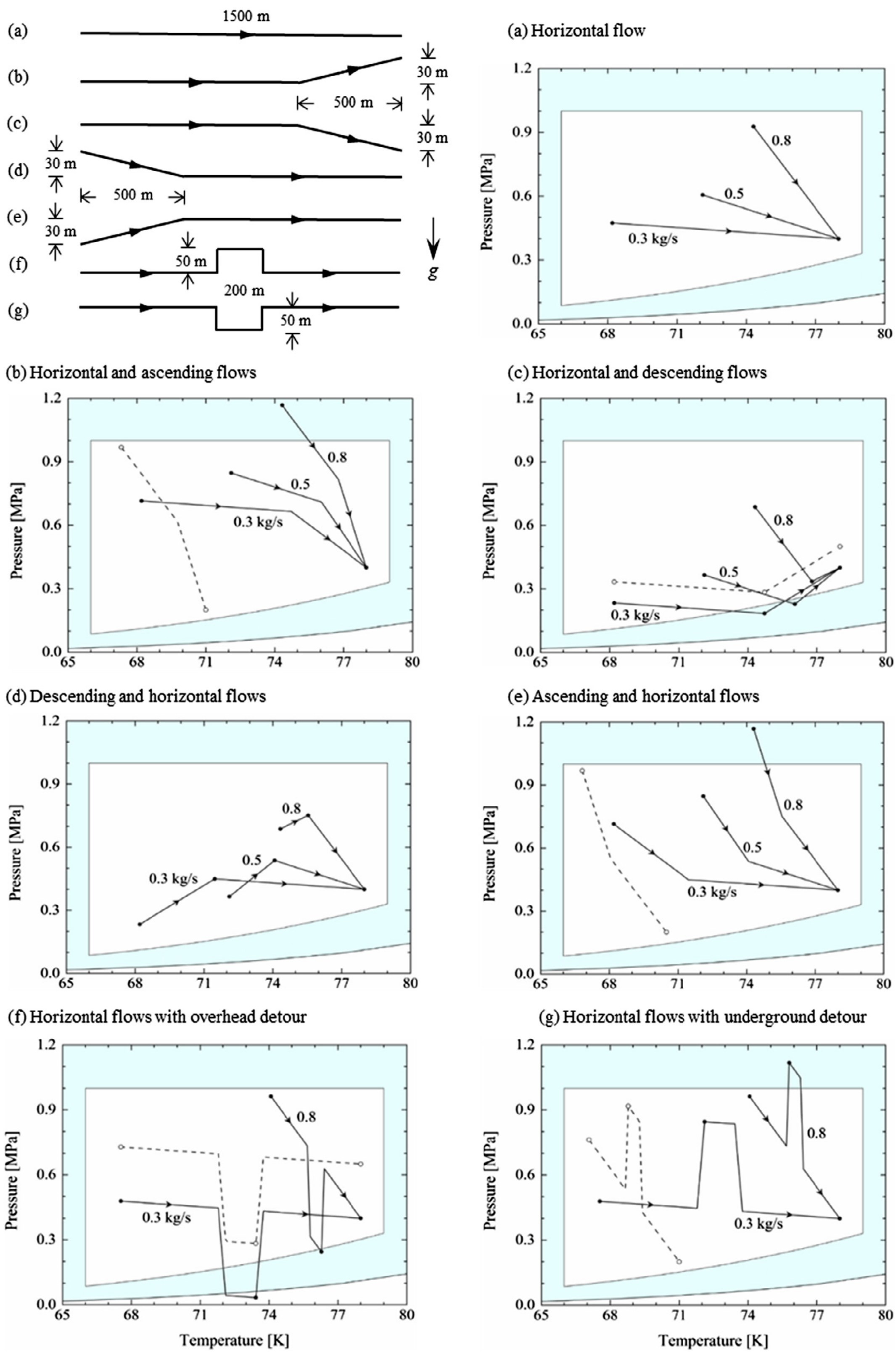

Fig. 5. Seven cases of simplified geographical layout with altitude variation and LN_2 process in HTS cable.

but at the ending point of descending section. In Case (e), the inlet pressure may be set at a higher value due to the ascending section. When the flow rate is 0.8 kg/s, the entire process should be shifted to left and down on phase diagram for safe operation, as indicated by dashed lines in Fig. 5(e).

In Case (f) and Case (g), the effect of overhead and underground detours is examined, respectively. When the flow rate is 0.3 kg/s, a higher inlet pressure is required for the overhead detour, as indicated by dashed lines in Fig. 5(f), but no substantial change is needed for the underground detour in Case (g). When the flow rate is 0.8 kg/s, on the other hand, the LN_2 process should be shifted to left and down on phase diagram for the underground detour, as indicated by dashed lines in Fig. 5(g), but no substantial change is needed for the overhead detour in Case (f). In all cases, the high pressure limit should be confirmed about the top flow in Case (f), while the sub-cooling margin should be confirmed about the bottom flow in Case (g), as indicated by the dots on the graphs in Fig. 5.

A few comments are made about the possible errors in the presented calculation caused by the simplified assumptions on LN_2 properties. The density and specific heat of LN_2 vary over the flow, but was assumed to be constant as the average values listed in Table 1. The temperature rise in real systems could be larger than calculated, because the pressure effect on enthalpy was not fully included in Eq. (2). The pressure drop in LN_2 flow is very important in momentum balance for the pumping requirement, but plays only a minor role (0.4–5%) of viscous dissipation in energy balance. The assumption of constant density is another source of error in the calculation of pressure drop. A numerical analysis was performed for some selected cases, taking into account the density variation with 100 divided segments of the cable length. The results show that the pressure drop could be lower than calculated in case of small flow (0.3 kg/s), but higher than calculated in case of large flow (0.8 kg/s). The objective of this work is to examine primarily the gravitational effect by altitude variation, and an elaborated numerical calculation with variable properties is recommended for more accurate analysis and design.

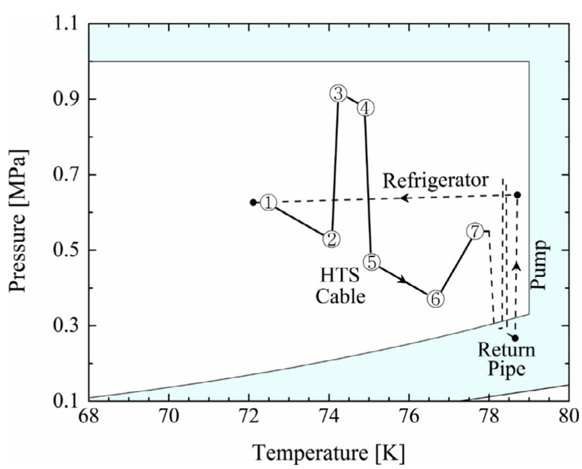

(a) Cooling facility at Terminal A (higher elevation) for A-B-A circulation (0.6 kg/s)

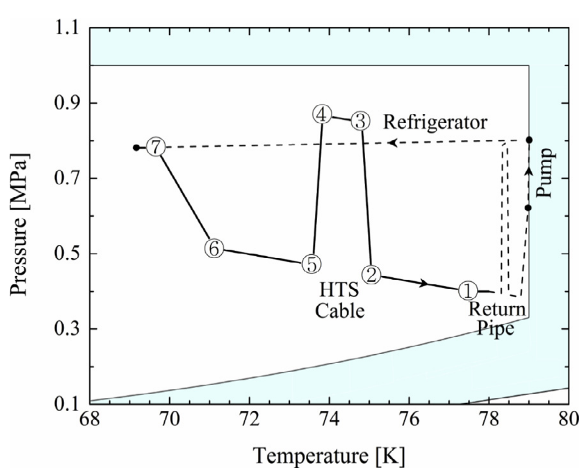

(b) Cooling facility at Terminal B (lower elevation) for B-A-B circulation (0.4 kg/s)

Fig. 6. Designed cycle of LN_2 circulation system for the geographic layout of HTS cable in Fig. 3.

3.3. An example of practical design

For the specific geographical layout shown in Fig. 3, the distribution of LN_2 pressure and temperature is calculated and plotted over the entire circulation loop (including the return pipe, LN_2 pump, and refrigerator) in Fig. 6. Two circulating directions are considered, depending on the location of the cooling facility building. Fig. 6(a) shows the case that the facility building is located at Terminal A (higher elevation) for A-B-A circulation, and Fig. 6(b) shows the other case that the facility building is located at Terminal B (lower elevation) for B-A-B circulation.

In Fig. 6(a), the first peak ②-③-④-⑤ represents the underground detour, and the line ⑥-⑦ represents the descending section. The LN_2 flow rate is 0.6 kg/s as discussed below, and the cooling requirements are satisfied for the entire process in HTS cable. The points of maximum (③) and minimum (⑥) pressure are securely fitted in the trapezoid. Similarly in Fig. 6(b), the line ⑦-⑥ represents the ascending section, and the peak ⑤-④-③-② represents the following underground detour. When compared with the operating conditions in Fig. 6(a), the inlet pressure should be higher and the inlet temperature should be lower. The LN_2 flow rate is 0.4 kg/s as discussed below, and the cooling requirements are also satisfied for the entire process in HTS cable. The points of maximum (④) and minimum (①) pressure are securely fitted in the trapezoid.

The LN_2 flow through the return pipe is plotted with dashed lines in both cases. The LN_2 state in the return pipe and pump may be outside the trapezoid on phase diagram, as far as it remains in sub-cooled liquid region. The sharp peak with the dashed lines represents the overhead or underground detour of the return pipe. The vertical upward line at right is the pump process, and the horizontal right-to-left line at top is the refrigeration process in the cooling facility building.

As mentioned above, the LN_2 flow rate should be carefully determined along with the range of pressure and temperature. In case of A-B-A circulation, the cooling requirements may be satisfied for any value of LN_2 flow rate between 0.3 and 0.8 kg/s. Fig. 6(a) shows the complete cycle when the flow rate is 0.6 kg/s. The LN_2 pressure and temperature are (0.63 MPa, 72.1 K) at terminal A, (0.92 MPa, 74.2 K) at ③, (0.37 MPa, 76.7 K) at ⑥, and (0.55 MPa, 78 K) at Terminal B. In case of B-A-B circulation, however, the flow rate should be selected only in the range of 0.3–0.6 kg/s in order to meet the cooling requirements. Fig. 6(b) shows the complete loop when the flow rate is 0.4 kg/s. The LN_2 pressure and temperature are (0.78 MPa, 69.1 K) at Terminal B, (0.87 MPa 73.8 K) at ④, and (0.4 MPa, 78 K) at Terminal A. It may be stated with this example that there is a wider design margin in the operational condition of LN_2, when the cooling facility is located at the higher elevation.

Table 2
Required specifications of LN_2 pump and cryogenic refrigerator.

		Fig. 6(a) A-B-A circulation	Fig. 6(b) B-A-B circulation
LN_2 pump	Flow rate	0.6 kg/s (44 L/min)	0.4 kg/s (29 L/min)
	Pumping head	0.38 MPa (4.8 m)	0.18 MPa (2.3 m)
Refrigerator	Cooling capacity	8.0 kW	8.0 kW
	Temperature	70.6 K	67.6 K

The required specifications of LN_2 pump and refrigerator are summarized in Table 2 for both cases. The A-B-A circulation in Fig. 6(a) needs a larger flow rate and pumping head than the B-A-B circulation in Fig. 6(b). A larger capacity of LN_2 pump must be employed for the circulation system shown in Fig. 6(a). On the other hand, the thermal load is basically identical for two cases, but the refrigeration temperature for the A-B-A circulation in Fig. 6(a) is approximately 3.0 K higher. The refrigeration temperature is assumed to be 1.5 K below the lowest LN_2 temperature, taking the heat exchange effectiveness into consideration [19]. The cooling capacity of Brayton refrigerators is strongly dependent on the refrigeration temperature in this operational range [11,18]. For example, a state-of-the-art Brayton refrigerator (10 kW at 77 K) should be capable of providing 8.0 kW at 70.6 K, but may not be enough to provide 8.0 kW at 67.6 K. As critically demonstrated in this example, the merits of higher-temperature refrigeration could play a major role in practical design.

4. Conclusion

A thermal and hydraulic study is presented to determine the cryogenic condition of LN_2 circulation system for long-length HTS cables with altitude variation. The cooling requirements are defined in terms of the pressure and temperature of LN_2, and it is demonstrated how the circulation loop on phase diagram can be used to confirm the requirements subject to given geographical constraints. We conclude that the LN_2 flow rate should be carefully determined together with the distribution of pressure and temperature along the circulation loop, and the proposed graphical method is useful in the cryogenic design.

Acknowledgments

This research is supported by a grant of the Korea Institute of Energy Technology Evaluation and Planning (KETEP) for Power Generation & Electricity Delivery Program (No. 2014 101050231B), funded by the Ministry of Trade, Industry and Energy of Korean Government.

Appendix A

The energy balance equation (including the gravitational potential energy) for a control volume having an inlet (i) and an exit (e) is written as

$$\frac{dE}{dt} = 0 = q + \dot{m}[(h_i - h_e) + g(z_i - z_e)] \tag{A1}$$

in steady state, if there is no work and no change in kinetic energy. For an incompressible fluid [20],

$$\begin{aligned} h_i - h_e &= \int_{T_e}^{T_i} C_p dT + \int_{P_e}^{P_i} \left[v - T\left(\frac{\partial v}{\partial T}\right)_P \right] dP \\ &\approx \int_{T_e}^{T_i} C_p dT + v(P_i - P_e) \end{aligned} \tag{A2}$$

which is substituted for the enthalpy difference in Eq. (A1).

$$0 = q + \dot{m}\left[\int_{T_e}^{T_i} C_p dT + v(P_i - P_e) + g(z_i - z_e)\right] \tag{A3}$$

The last two parenthesis terms represent the pressure effect and the elevation effect, which are eliminated by the momentum (i.e. Bernoulli) equation.

$$q = \dot{m}\int_{T_i}^{T_e} C_p dT \approx \dot{m}C_p(T_e - T_i) \tag{A4}$$

if the minor viscous dissipation is neglected or included as part of the heat load.

References

[1] Yumura H, Ashibe Y, Ohya M, Itoh H, Watanabe M, Masuda T, et al. Status of YOKOHAMA HTS cable project. IEEE Trans Appl Supercond 2013;23:5402306.
[2] Nakano T, Maruyama O, Honjo S, Watanabe M, Masuda T, Hirose M, et al. Long-term operating characteristics of Japan's first in-grid HTS power cable. Physica C 2015;518:126–9.
[3] Sytnikov VE, Bemert SE, Kopylov MA, Romashov MA, Ryabin TV, Shakaryan YG, et al. Status of HTS cable link project for St. Petersburg grid. IEEE Trans Appl Supercond 2015;25:5400904.
[4] Herzog F, Kutz T, Stemmle M, Kugel T. Cooling unit for the AmpaCity – one year of successful operation. Cryogenics 2016;80:204–9.
[5] Xiao L, Dai S, Lin L, Teng Y, Zhang H, Liang X, et al. Development of a 10 kA HTS DC power cable. IEEE Trans Appl Supercond 2012;22:5800404.
[6] Sohn SH, Yang HS, Lim JH, Oh SR, Yim SW, Lee SK, et al. Installation and power grid demonstration of a 22.9 kV, 50 MVA, high temperature superconducting cable for KEPCO. IEEE Trans Appl Supercond 2012;22:5800804.
[7] Yang B, Kang J, Lee S, Choi C, Moon Y. Qualification test of a 80 kV 500 MW HTS dc cable for applying into real grid. IEEE Trans Appl Supercond 2015;25:5402705.
[8] Chang HM, Ryu KN, Yang HS. Integrated design of cryogenic refrigerator and liquid-nitrogen circulation loop for HTS cable. Cryogenics 2016;80:183–92.
[9] Demko JA, Hassenzahl WV. Thermal management of long-length HTS cable systems. IEEE Trans Appl Supercond 2011;21:957–60.
[10] Nam K, Seok BY, Byun JJ, Chang HM. Suppression of bubbles in subcooled liquid nitrogen under heat impulse. Cryogenics 2007;47:442–9.
[11] Yoshida S, Hirai H, Nara N, Ozaki S, Hirokawa M, Eguchi T, et al. Sub-cooled liquid nitrogen cryogenic system with neon turbo-refrigerator for HTS power equipment. Adv Cryog Eng 2014;1573:1246–53.
[12] Chang HM, Gwak KH, Yang HS, Hwang SD. Cross-flow heat changers for anti-freezing of liquid nitrogen. Cryogenics 2013;57:122–8.
[13] Weisend JG. Handbook of cryogenic engineering. Philadelphia: Taylor & Francis; 1998.
[14] Ivanov Y, Watanabe H, Hamabe M, Kawahara T, Sun J, Yamaguchi S. Design study of LN_2 circulation in a long SC power transmission lines. Phys Proc 2012;36:1372–7.
[15] Weisend JG, Van Sciver SW. Pressure drop from flow of cryogens in corrugated bellows. Cryogenics 1990;30:935–41.
[16] Watanabe H, Ivanov YV, Hamabe M, Chikumoto N, Kawahara T, Kakano H, et al. Circulation test of liquid nitrogen for long superconducting dc power transmission lines. IEEE Trans Appl Supercond 2016;26:5400504.
[17] Lemmon EW, Huber ML, McLinden MO. NIST Reference Fluid Thermodynamic and Transport Properties Database REFPROP Version 9.0, <https://www.nist.gov/srd/refprop>.
[18] Hirai H, Hirokawa M, Yoshida S, Sano T, Ozaki S. Development of a turbine-compressor for 10 kW class neon turbo-Brayton refrigerator. Adv Cryog Eng 2014;1573:1236–41.
[19] Chang HM, Gwak KH, Jung S, Yang HS, Hwang SD. Plate-fin heat-exchangers for a 10 kW Brayton cryocooler and a 1 km HTS cable. Phys Proc 2015;67:221–6.
[20] Bejan A. Advanced engineering thermodynamics. 3rd ed. New York: John Wiley & Sons; 2006.